Differential Strategy to High-Speed Inspection of Rails Via Passive Ultrasonic Monitoring

IZABELA C. BATISTA, ALI ZARE HOSSEINZADEH,
DIPTOJIT DATTA and FRANCESCO LANZA DI SCALEA

ABSTRACT

This work presents an amplitude-imbalance identification approach to noncontact high-speed rail inspections. The passive monitoring utilizes an array of capacitive air-coupled ultrasonic transducers for data acquisition of ultrasonic-guided waves propagating in the rail. The excitation is generated by a combination of the test car's wheel-rail friction and white noise generated by two additional actuators. The transfer function is reconstructed passively between two air-coupled sensors and transformed to the time domain by deconvolution. When discontinuities are present in the rail, the signature waveform in the time domain transfer function will change due to scattering. These changes in the amplitude of the reconstructed signal can be associated with the potential presence of a flaw. This method is referred to as the conventional approach to defect detection. However, tracking changes in one waveform is still subject to variability due to changing test conditions, different rail geometries, wear, poorer signal strength, and other rail anomalies that may be falsely flagged as defects. This paper presents a more robust defect detection strategy achieved by simultaneously assessing amplitude-related features from time signals of two sensors pairs probing adjacent segments of rail and using any significant mismatch as the indicator of an internal rail flaw in one of the two segments, hence, the differential strategy for defect detection. The performance of such a method in detecting flaws was assessed via receiver operating characteristic curves on data acquired from field tests at testing speeds of 40 mph conducted at the Transportation Technology Center Inc (TTCI) in Pueblo, CO.

INTRODUCTION

Defective rails are a major concern for the railroad industry, as they can have a significant impact on safety and operations. The main causes of defective rails are transverse defects and detail fractures, which are primarily caused by manufacturing defects and rolling contact fatigue. Although advancements have been made to reduce these issues, internal defects remain a major concern in the railroad industry.

Izabela C. Batista; Ali Zare Hosseinzadeh; Francesco Lanza di Scalea, University of California San Diego, 9500 Gilman Drive, La Jolla, CA 92093, U.S.A.
Diptojit Datta, Exponent Inc., 1331 17th Street #515, Denver, CO 80202, U.S.A.

The current industry standards for detection of rail flaws involve ultrasonic tests conducted by Rolling Search Units (RSUs), which are fluid-filled tires with piezoelectric transducers that roll along a rail. However, RSUs are limited to operating at a maximum of 30 mph, a value much lower than revenue speeds, requiring careful scheduling to minimize traffic disruptions.

To address the limitations of the existing ultrasonic rail inspection techniques, a high-speed passive noncontact ultrasonic rail inspection technique has been proposed [1]. The technique uses capacitive air-coupled ultrasonic transducers for the continuous data acquisition of ultrasonic-guided waves propagating in the rail. The data is then processed to extract the rail's transfer function. The technique takes advantage of the wheel-generated excitation, boosted by white noise emitters, to estimate the system's transfer function in an output-only approach. In the time domain, amplitude-related features are extracted from the characteristic waveform. If discontinuities are present in the rail, these features will track changes in the waveforms caused by wave scattering.

The conventional approach of using features from a single waveform to track anomalies in a dataset has been extensively explored in the past [2]. However, this method is often affected by operational variability, such as changes in test conditions, different rail geometries, rail wear, and signal strength, all of which may cause pristine data to be falsely labeled as defective.

This paper proposes a more robust defect detection methodology by using a differential strategy. This strategy consists of assessing features from signals of two pairs of sensors probing adjacent segments of rail simultaneously. Any significant mismatch between the two signals can be used as an indicator of an internal rail flaw in one of the two segments. A statistical outlier analysis will be used to detect two types of discontinuities: transverse defects and jointed rail sections. The anomaly detector performance will be evaluated by varying the threshold level and computing the receiver operating characteristic (ROC) curves on data acquired at the Transportation and Technology Center Inc. (TTCI) at a train travel speed of 40 mph.

DUAL-OUTPUT TRANSFER FUNCTION RECONSTRUCTION

A linear model was proposed to represent the wheel-rail dynamic interaction [3], as shown in Figure 1. In this model, the rail is excited by the friction of the rolling wheel, $E(\omega)$. A pair of air-coupled sensors probe the rail response to the input at locations A and B. The frequency response, $O_A(\omega)$, is the result of the combination of the transfer function representing the segment between the wheel position and the sensor A, $EA(\omega)$, and noise measured at the sensor A, $N_A(\omega)$. The frequency response $O_B(\omega)$ is the transfer function representing the rail segment between sensors A and B, $G_{AB}(\omega)$ embedded with the noise measured at sensor B, $N_B(\omega)$.

The robust passive reconstruction of the transfer function $G_{AB}(\omega)$ is computed by the normalized cross-power spectrum operation between $O_A(\omega)$ and $O_B(\omega)$:

$$G_{AB}(\omega) = \frac{<\text{CPSD}>_{intra-segment}}{<\text{PSD}>_{inter-segment}} = \frac{<O_A^*(\omega) \cdot O_B(\omega)>_{intra-segment}}{<O_A^*(\omega) \cdot O_A(\omega)>_{inter-segment}}, \quad (1)$$

and converted to the time domain ($g_{AB}(t)$) via inverse Fourier Transform.

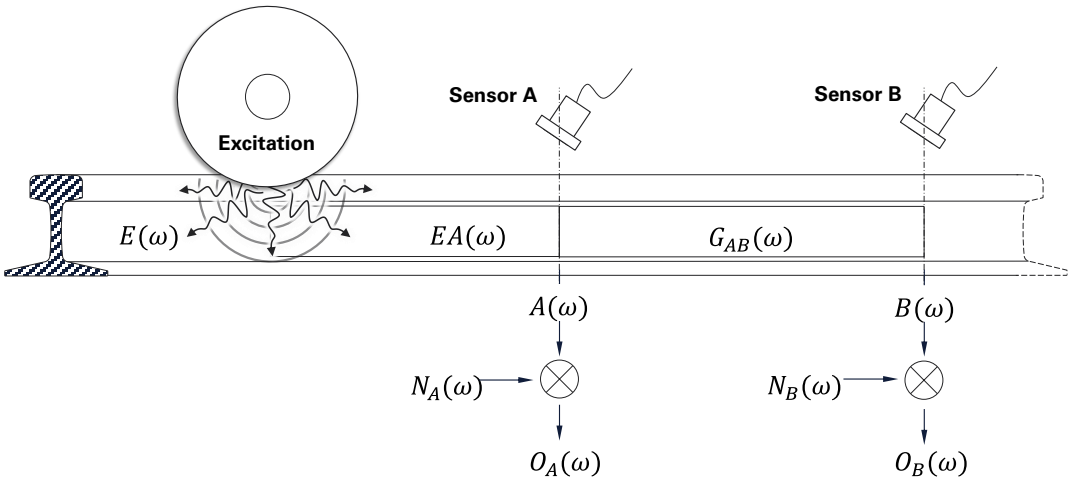

Figure 1. Rail dual-output transfer function reconstruction schematics.

SIGNAL PROCESSING

Figure 2(a) shows a sample of the data acquired from a pair of sensors positioned 18 inches apart. The transfer function and impulse response were computed from these signals and are shown in Figure 2(b) and (c), respectively. The signature waveform is often observed at two different instances: approximately 140 microseconds for wave packets in the range 20 and 40 kHz, and approximately 160 microseconds for signals between 70 and 120 kHz [3]. These wave signals correspond to a combination of flexural and torsional ultrasonic guided waves being excited by the train wheel and propagating between the two transducers through the rail.

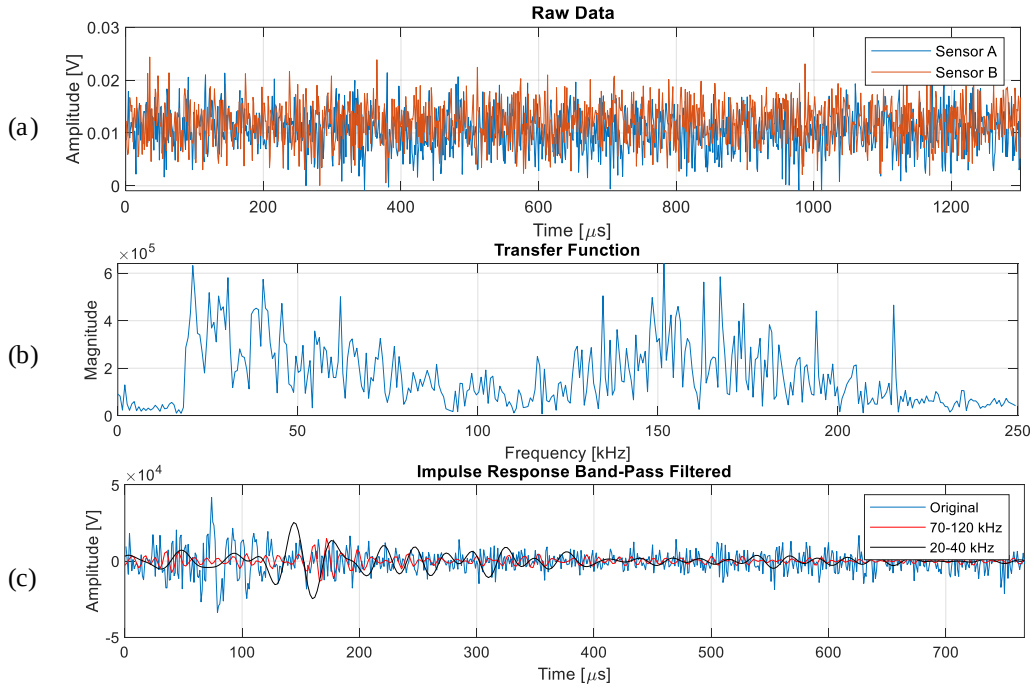

Figure 2. Sample of (a) the raw data acquired at two different transducers, (b) the transfer function frequency components and (c) the impulse response filter under different frequency bands.

EXPERIMENTAL SETUP AND FIELD TEST

A passive rail inspection prototype was attached to the Federal Railroad Administration 5229 Test Car at the TTCI in Pueblo, CO, as shown in Figure 3. The prototype consisted of 12 ultrasonic capacitive air-coupled transducers. The transducers were positioned at a minimum lift-off of 3 inches from the rail's top surface to guarantee true noncontact probing of the rail. The transducers were angled at 6 degrees to maximize the receiving of leaky waves propagating in the railhead. A laser system was used to ensure that the transducers were aligned with the rail. Two additional capacitive air-coupled transducers were used to send Gaussian white noise to enhance the signal-to-noise ratio (SNR) of the acquired signals throughout the tests. A camera captured images of the rail during the tests to detect the presence of welds, joints, and marked defects, enabling the creation of a ground truth. A global positioning system (GPS) receiver was mounted on the top of the test car, synchronizing the signal collected and images to the same geographical position.

The test was performed at 40 mph, the maximum allowed speed on the High-Tonnage Loop (HTL). Three laps were performed at this 2.7-mile track: two laps with the white noise emitters turned on and one lap with the emitters turned off. The HTL track had 8 known natural transverse defect locations and 10 joints.

The data acquisition system used in the field tests comprised of:

(1) National Instruments (NI) PCI and PXIe unit running LabView real-time for data recording and processing.
(2) Tachometer transistor-transistor logic (TTL) pulse for spatial positioning of the test car, with a spatial resolution of 1.6 inch.
(3) High-speed SONY ICX-424 camera with a 6mm C-mount lens and maximum frame rate of 100 frames per second.
(4) Stroboscopic LED light of 30k Lumens for appropriate illumination.
(5) NovAtel's FlexPak 6D Global Navigation Satellite System (GNSS) receiver.
(6) Windows 10 computer connected to the PXIe unit.

The signals from the air-coupled transducers were recorded continuously at a 1 MHz sampling frequency. The camera captured images at 100 frames per second, and the GPS positions were recorded at 10 Hz.

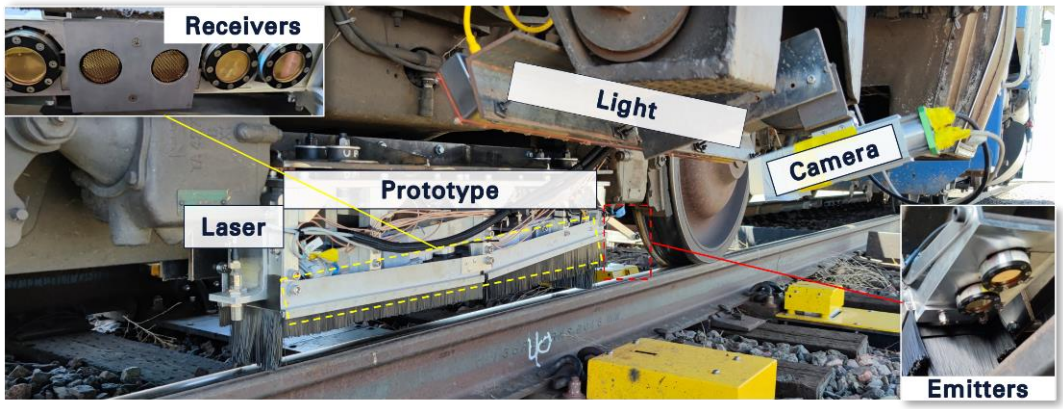

Figure 3. Passive inspection prototype mounted to the test car at TTCI.

STATISTICAL OUTLIER ANALYSIS

Variations in the impulse response are tracked statistically by a statistical outlier analysis. Discontinuity-sensitive features, such as the variance, skewness, and kurtosis, are extracted from the time signals and concatenated in a feature vector $\boldsymbol{x}$. The Damage Index (DI) of each probed rail segment is computed using the Mahalanobis Squared Distance (MSD) metric

$$\mathrm{DI} = (\boldsymbol{x} - \overline{\boldsymbol{x}})^{\mathrm{T}} \cdot \mathbf{Cov}^{-1} \cdot (\boldsymbol{x} - \overline{\boldsymbol{x}}) \tag{2}$$

where $\overline{\boldsymbol{x}}$ is the mean value of the features on the pristine baseline and $\mathbf{Cov}$ is the respective covariance matrix. Outliers are flagged when a DI value above a certain threshold is returned, thus suggesting a possible discontinuity presence. Analogously, a DI value below the threshold is an indicative of a pristine rail segment.

In the conventional approach, the multi-variate feature array $\boldsymbol{x}$ is constructed by extracting the previously mentioned features from 6 impulse responses, (one from each sensor pair), and gathering them in a matrix $\boldsymbol{x}$ of M probed rail locations by N features of interest:

$$\boldsymbol{x}_{\mathrm{Conventional}} = \left[\begin{Bmatrix} \mathrm{feature}_1[\{g_{AB}(t), g_{CD}(t), \dots\}] \\ \mathrm{feature}_2[\{g_{AB}(t), g_{CD}(t), \dots\}] \\ \dots \\ \mathrm{feature}_{\mathrm{N}}[\{g_{AB}(t), g_{CD}(t), \dots\}] \end{Bmatrix}_{\substack{\mathrm{segment} \\ 1}} \dots \begin{Bmatrix} \dots \\ \dots \\ \dots \\ \dots \end{Bmatrix}_{\substack{\mathrm{segment} \\ \mathrm{M}}} \right]^T \tag{3}$$

Then, the DI trace is computed. However, the scale of these features tends to vary significantly as the operational conditions change, causing pristine rail sections under atypical operational conditions to be falsely flagged as defective.

The "differential" strategy proposed to overcome the effect of such changes on the features was implemented by computing the ratio between the features from signals of neighbor sensor pairs probed synchronously:

$$\boldsymbol{x}_{\mathrm{Differential}} = \left[\begin{Bmatrix} \frac{\mathrm{feature}_1[g_{AB}(t)]}{\mathrm{feature}_1[g_{CD}(t)]}, \frac{\mathrm{feature}_1[g_{EF}(t)]}{\mathrm{feature}_1[g_{GH}(t)]} \dots \\ \frac{\mathrm{feature}_2[g_{AB}(t)]}{\mathrm{feature}_2[g_{CD}(t)]}, \frac{\mathrm{feature}_2[g_{EF}(t)]}{\mathrm{feature}_2[g_{GH}(t)]} \dots \\ \dots \\ \frac{\mathrm{feature}_{\mathrm{N}}[g_{AB}(t)]}{\mathrm{feature}_{\mathrm{N}}[g_{CD}(t)]}, \frac{\mathrm{feature}_{\mathrm{N}}[g_{EF}(t)]}{\mathrm{feature}_{\mathrm{N}}[g_{GH}(t)]} \dots \end{Bmatrix}_{\substack{\mathrm{segment} \\ 1}} \dots \begin{Bmatrix} \dots \\ \dots \\ \dots \\ \dots \end{Bmatrix}_{\substack{\mathrm{segment} \\ \mathrm{M}}} \right]^T . \tag{4}$$

RECEIVER OPERATING CHARACTERISTIC CURVES

The ROC curve is a graphical plot of the true positive rate (TPR) against the false positive rate (FPR), calculated as the threshold value of the DI's cutoff is varied. The TPR, also referred to as Probability of Detection (PoD), is the proportion of the defective rail that was correctly identified as damaged:

$$\mathrm{PoD} = \frac{\mathrm{Number\ of\ discontinuities\ detected}}{\mathrm{Total\ number\ of\ discontinuities\ in\ the\ test\ track}}. \tag{5}$$

The FPR, also known as Probability of False Alarms (PFA), is the proportion of the pristine rail that was incorrectly identified as damaged:

$$\mathrm{PFA} = \frac{\text{Number of discontinuities erroneously detected}}{\text{Total number pristine segments in the test track}}. \quad (6)$$

The ROC curve is used to evaluate the performance of a monitoring system in detecting discontinuities. A perfect inspection system would result in a ROC curve that lies in the top left corner of the plot, with a total area under the curve (AUC) of 1. A good inspection system would be as close to these standards as possible, with high PoD and low PFA values for a variety of threshold levels.

To compute the ROC curve, the track is segmented into pristine and defective rail segments (enclosing welds, joints, and transverse defects). Notice that the transversal defects are internal, but they have been located by the inspection personnel at TTCI and their respective rail segments were painted, so that they could be visually identified. The certainty around the position of the defective sections is subject to many unknowns, such as the observability of the rail feature on the acquired images, the capability of the image processing algorithms to correctly classify the rail features for the ground truth creation, the GPS precision, data fusion and synchronization between all different sensors in monitoring system. To overcome these uncertainties, a safety margin around defective segments is discarded so that the discretized pristine rail segments contain only data unaffected by discontinuities. The same steps are taken towards the defective population so that pristine rail segments are not accounted for as defective.

The number of discontinuities detected is computed by observing the number of times that the DI exceeds the threshold within the scanning length of the prototype (1.5 ft). The 1.5 ft probed segment is deemed defective if a minimum number of threshold crossing (NTC) is observed from the DI values encompassing that region. Therefore, if this event is observed within the defective population, this is a true positive detection, whereas if this event is observed on the pristine population, it is a false alarm.

Multiple passes over the same segment of rail, as in normal traffic operations, can be used to minimize the FPR. Only detections that are consistently flagged over multiple probing attempts are likely to be actual discontinuities. Hence, redundancy is expected to improve the detection performance of the monitoring system [4]. An example of the improvement of classifying the data after two observations of the rail track is exemplified in Figure 4.

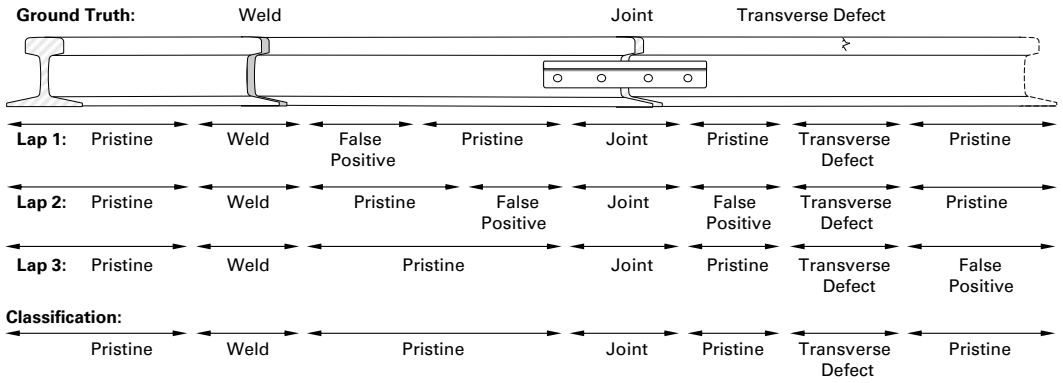

Figure 4. Segregation between pristine, welded, bolted joints, and defective rail sections on the ground truth, classification of the first run (lap 1), classification of the second run (lap 2), classification of the third run (lap 3), and redundant classification of the rail track using all runs combined.

FIELD TEST RESULTS

Figures 5 and 6 compare the detection performance when using the conventional and differential strategies. They present the ROC curves for two different runs (noise emitter on and off) at the HTL test track at 40 mph. The curves observed are:

a) Single lap with white noise emitters turned off (orange line).
b) First lap with white noise emitters turned on (purple line).
c) Second lap with white noise emitters turned on (green line).
d) Redundancy test on first and second laps compounded with white noise emitters turned on (thick blue line).
e) Redundancy test on first and second laps with white noise emitters turned on, and single lap with emitters turned off compounded (thick black line).
f) A random guess – the TPR and TFR are equal same for all threshold values (dashed black line)

The discontinuity safety margin used was 1.5 ft. The discontinuity search area encompassed ± 15 ft to compute the number of times that the DI values crossed the threshold [4].

For the classification of joints presented in Figure 5, none of the strategies appear to be more advantageous than the other, as the performance of both detectors are very similar: 18% PFA at 100% PoD for the differential approach *versus* 16% PFA at 100% PoD for the conventional approach for all laps combined, and both strategies yielded approximately 0.95 AUC.

However, in terms of detecting internal flaws, the differential strategy has a much superior performance than the conventional strategy, as shown in Figure 6. When compounding all three laps, the differential strategy yielded a 6% PFA at 100% PoD, while the conventional strategy yielded a much higher PFA of 27% at 100% PoD. In addition, the AUC from the differential approach is approximately 0.97 whereas the AUC from the conventional approach is 0.92.

Finally, the importance of redundancy is a common aspect in all 4 ROC curves shown in Figure 5 and 6, as the detector's performance improved significantly when multiple passes over the rail were considered.

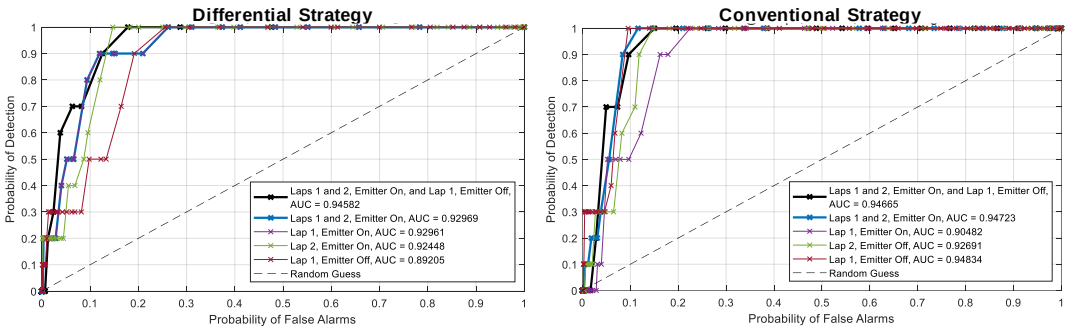

(a) (b)

Figure 5. ROC curves for joints on the HTL track at testing speed of 40 mph for a discontinuity search tolerance of ± 15ft comparing the detection using the (a) Differential and (b) Conventional Strategies.

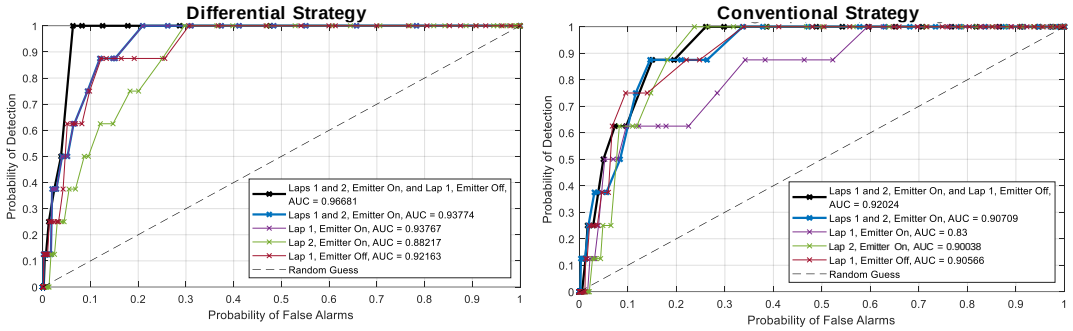

(a) (b)

Figure 6. ROC curves for transverse defect detection on the HTL track at testing speed of 40 mph for a discontinuity search tolerance of $\pm$15ft comparing the detection using the (a) Differential Strategy and (b) Conventional Strategy.

CONCLUSIONS

This study presented preliminary results of a new approach, the differential strategy, to manipulate features from the impulse responses. These results were compared to the already established conventional approach. To detect joints, both methods produced similar results, with the conventional one producing a 2% lower PFA. To detect defects, however, the differential strategy provided a 21% lower PFA at 100% POD when compared to the conventional strategy, proving that this new approach is feasible to be explored using other comparative techniques more complex than the features' ratio, other features, and datasets from other tests.

In addition, it was shown that a redundancy analysis when multiple passes over the same rail is available is essential for the success of the discontinuity detectors, such as the one presented in this work. The discontinuities detectors are expected to become more robust when compounding more passes over the rail, especially if the train test speed increases (better SNR) and the train's running direction changes, changing the UWG propagation direction.

ACKNOWLEDGMENT

This project was funded by the Federal Railroad Administration (Contract #693JJ620C000024).

REFERENCES

1. Lanza di Scalea, F., Rizzo, P., Coccia, S., Bartoli, I., Fateh, M., Viola, E., & Pascale, G. 2005. "Non-contact ultrasonic inspection of rails and signal processing for automatic defect detection and classification". *Insight-Non-Destructive Testing and Condition Monitoring*, *47*(6), 346-353.
2. Mariani, S., & di Scalea, F. L. 2018. "Predictions of defect detection performance of air-coupled ultrasonic rail inspection system". *Structural Health Monitoring*, *17*(3), 684-705
3. Di Scalea, F. L., Liang, A. Y. L., Sternini, S., Capriotti, M., Datta, D., Zhu, X., & Wilson, R. 2019. "Ultrasonic identification of rail tracks from natural wheel excitations: potential for high-speed and high-redundancy rail inspection". *Structural Health Monitoring 2019*.
4. Datta, D. & Lanza di Scalea, F. (2022). "High-Speed Inspection of Rails by Passive Ultrasonic Monitoring". *Journal of Nondestructive Evaluation, Diagnostics and Prognostics of Engineering Systems*, *5*(4), 041007.